# Nonlinear optical waveguides based on near-infrared intersubband transitions in GaN/AlN quantum wells

**Yan Li, Anirban Bhattacharyya, Christos Thomidis, Theodore D. Moustakas, and Roberto Paiella**

*Department of Electrical and Computer Engineering and Photonics Center,*
*Boston University, Boston, MA 02215*
*rpaiella@bu.edu*

**Abstract:** We present the design, fabrication, and characterization of III-nitride quantum-well waveguides optimized for nonlinear-optical switching via intersubband transitions. A dielectric structure consisting of an AlN lower cladding and a GaN cap layer allows minimizing the propagation losses while maintaining a large modal overlap with the quantum-well active layer. A strong nonlinear saturation of the intersubband absorption near 1.55 μm is demonstrated at record low input powers for these materials; in particular, a 3-dB saturation pulse energy of less than 10 pJ with 240-fs pulses is measured. Combined with the well established sub-picosecond recovery lifetimes of intersubband absorption in III-nitride quantum wells, these results are very promising for all-optical switching applications in future ultrafast fiber-optic communication networks.

## References and links

1. A. V. Gopal, H. Yoshida, A. Neogi, N. Georgiev, T. Mozume, T. Simoyama, O. Wada, and H. Ishikawa, "Intersubband absorption saturation in InGaAs-AlAsSb quantum wells," IEEE J. Quantum Electron. **38**, 1515-1520 (2002).
2. R. Akimoto, B. S. Li, K. Akita, and T. Hasama, "Subpicosecond saturation of intersubband absorption in (CdS/ZnSe)/BeTe quantum well waveguides at telecommunication wavelength," Appl. Phys. Lett. **87,** 181104 (2005).
3. C. Gmachl, H. M. Ng, S.-N. G. Chu, and A. Y. Cho, "Intersubband absorption at λ ~ 1.55 μm in well- and modulation-doped GaN/AlGaN multiple quantum wells with superlattice barriers," Appl. Phys. Lett. **77**, 3722-3724 (2000).
4. N. Iizuka, K. Kaneko, and N. Suzuki, "Near-infrared intersubband absorption in GaN/AlN quantum wells grown by molecular beam epitaxy," Appl. Phys. Lett. **81**, 1803-1805 (2002).
5. Q. Zhou, J. Chen, B. Pattada, M. O. Manasreh, F. Xiu, S. Puntigan, L. He, and K. S. Ramaiah, and H. Morkoç, "Infrared optical absorbance of intersubband transitions in GaN/AlGaN multiple quantum well structures," J. Appl. Phys. **93**, 10140-10142 (2003).
6. R. Rapaport, G. Chen, O. Mitrofanov, C. Gmachl, H. M. Ng, and S. N. G. Chu, "Resonant optical nonlinearities from intersubband transitions in GaN/AlN quantum wells," Appl. Phys. Lett. **83**, 263-265 (2003).
7. J. Hamazaki, S. Matsui, H. Kunugita, K. Ema, H. Kanazawa, T. Tachibana, A. Kikuchi, and K. Kishino, "Ultrafast intersubband relaxation and nonlinear susceptibility at 1.55 μm in GaN/AlN multiple-quantum wells," Appl. Phys. Lett. **84**, 1102-1104 (2004).
8. I. Friel, K. Driscoll, E. Kulenica, M. Dutta, R. Paiella, and T. D. Moustakas, "Investigation of the design parameters of AlN/GaN multiple quantum wells grown by molecular beam epitaxy for intersubband absorption," J. Cryst. Growth **278**, 387-392 (2005).
9. L. Nevou, M. Tchernycheva, L. Doyennette, F. H. Julien, E. Warde, R. Colombelli, F. Guillot, S. Leconte, E. Monroy, T. Remmele, and M. Albrecht, "New developments for nitride unipolar devices at 1.3-1.5 μm wavelengths," Superlattices Microstruct. **40**, 412-417 (2006).
10. D. Hofstetter, S.-S. Schad, H. Wu, W.J. Schaff, and L.F. Eastman, "GaN/AlN-based quantum-well infrared photodetector for 1.55 μm," Appl. Phys. Lett. **83**, 572-574 (2003).

11. N. Iizuka, K. Kaneko, and N. Suzuki, "Sub-picosecond all-optical gate utilizing an intersubband transition," Opt. Express **13**, 3835-3840 (2005).
12. N. Iizuka, K. Kaneko, and N. Suzuki, "All-optical switch utilizing intersubband transition in GaN quantum wells," IEEE J. Quantum Electron. **42**, 765-771 (2006).
13. L. Nevou, F. H. Julien, R. Colombelli, F. Guillot, and E. Monroy, "Room-temperature intersubband emission of GaN/AlN quantum wells at $\lambda$=2.3 µm," Electron. Lett. **42**, 1308-1309 (2006).
14. G. Sun, J. B. Khurgin, and R. A. Soref, "Nonlinear all-optical GaN/AlGaN multi-quantum-well devices for 100 Gb/s applications at $\lambda$ = 1.55 µm," Appl. Phys. Lett. **87**, 201108 (2005).
15. Y. Li and R. Paiella, "Intersubband all-optical switching based on Coulomb-induced optical nonlinearities in GaN/AlGaN coupled quantum wells," Semicond. Sci. Technol. **21**, 1105-1110 (2006).
16. R. Hui, Y. Wan, J. Li, S. X. Jin, J. Y. Lin, and H. X. Jiang, "III-nitride-based planar lightwave circuits for long wavelength optical communications," IEEE J. Quantum Electron. **41**, 100-110 (2005).
17. O. Ambacher, B. Foutz, J. Smart, J. R. Shealy, N. G. Weimann, K. Chu, M. Murphy, A. J. Sierakowski, W. J. Schaff, L. F. Eastman, R. Dimitrov, A. Mitchell, and M. Stutzmann, "Two dimensional electron gases induced by spontaneous and piezoelectric polarization in undoped and doped AlGaN/GaN heterostructures," J. Appl. Phys. **87**, 334-344 (2000).

## 1. Introduction

Intersubband (ISB) transitions in semiconductor quantum wells (QWs) have found several device applications in the mid- and far-infrared spectral regions, including quantum-well infrared photodetectors and quantum cascade lasers. Due to their (sub)-picosecond relaxation lifetimes and large optical nonlinearities, these transitions are also promising for the development of ultrafast all-optical modulators and switches. These devices are expected to play a particularly important role in applications such as ultra-broadband signal processing and all-optical networking in fiber-optic communication systems, for which near-infrared operation wavelengths near 1.55 µm are required. Material systems with sufficiently large conduction-band offsets to accommodate ISB transitions at these relatively short wavelengths include InGaAs/AlAsSb [1], (CdS/ZnSe)/BeTe [2], and GaN/Al(Ga)N QWs [3-13].

In the past several years, the latter system in particular has been the subject of extensive research for these applications. Specific advantages of III-nitride semiconductors for ISB all-optical switching include their highly polar nature, which results in a very strong electron-LO phonon coupling and hence particularly fast ISB relaxation lifetimes, and their very wide bandgap, which precludes interband two-photon absorption of near-infrared light. Recently ISB absorption near 1.55 µm has been measured in various GaN/Al(Ga)N QW systems [3-9], followed by the demonstration of photodetection [10], all-optical switching by cross-absorption saturation [11-12], and optically pumped light emission [13] with similar structures. In addition, several pump-probe measurements in both unprocessed and waveguide samples have fully established the particularly fast nature of ISB relaxation in GaN/Al(Ga)N QWs, with measured lifetimes in the range 140-500 fs [6,7,11,12].

At the same time, however, relatively large ISB absorption saturation powers have also been observed, largely due to the broad ISB absorption linewidths of these QWs (typically ~ 100 meV). Using as a figure of merit the input power required to saturate the overall transmission losses by a factor of 2, the smallest value reported so far with waveguide devices is a 3-dB saturation peak power of approximately 190 W [12]. This important parameter can be improved through the design of both the nonlinear medium (e.g. using coupled QWs as described in recent theoretical studies [14, 15]) and the waveguide. The latter approach has so far received limited attention, with only one waveguide design used in these measurements. Here we report the design, fabrication, and testing of GaN/AlN QW waveguides exhibiting record low ISB saturation peak powers of ~ 42 W at wavelengths near 1.55 µm.

## 2. Design, growth, and fabrication

The QW material used in this work was grown by molecular beam epitaxy (MBE) on c-plane sapphire substrates, and consists of a 1.5-µm-thick AlN lower cladding layer, 30 repetitions of 18-Å-thick GaN wells and 40-Å-thick AlN barriers, and a 0.6-µm-thick GaN cap layer. Ridge waveguides of different widths were fabricated with this material by etching through the

entire thickness of the GaN cap. A scanning electron microscopy (SEM) image of the facet of a fabricated device is shown in Fig. 1(a). In these devices the guided modes are confined in the higher-index GaN upper layer, and thus they overlap with the QW active region through their evanescent tail into the lower cladding. By contrast, in the III-nitride QW waveguides previously developed to demonstrate ISB absorption saturation and switching, GaN is used in both the lower cladding and the cap layer, and the optical modes are confined between the GaN/sapphire and the GaN/air interfaces [11,12].
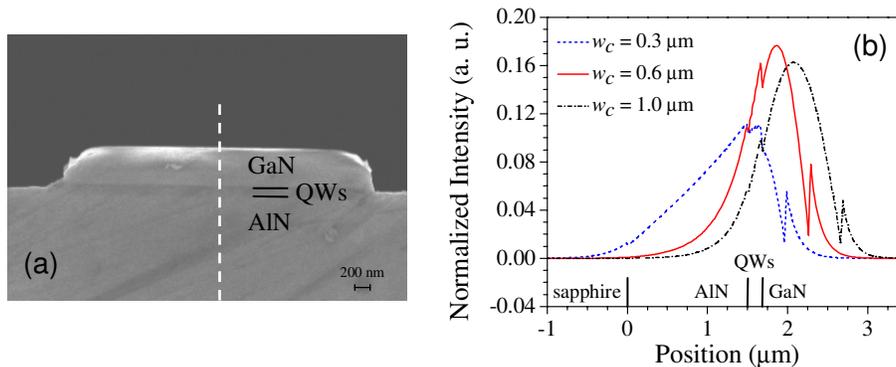


Fig. 1. (a). SEM image of the facet of a GaN/AlN QW waveguide. (b) Intensity profile of the fundamental TM mode along the dashed line of (a), for different thicknesses of the GaN cap.

The present design was motivated by several considerations. First, it minimizes the overlap between the optical modes and the first few tens of nm of epitaxial material near the sapphire substrate, where a very high density of dislocations exist due to the lattice and thermal mismatch between sapphire and (Al)(Ga)N. These structural defects, whose density rapidly decreases with distance from the substrate, have been found to provide a substantial contribution to the propagation losses in III-nitride waveguides, especially for TM light [12]. The use of a lower-index AlN layer below the QWs is therefore advantageous to reduce this non-saturable contribution to the waveguide losses. Incidentally, similar waveguides but without any QWs have also been studied recently for integrated-optics applications [16]. Second, the thickness of the GaN cap layer $w_c$ was selected to maximize the overlap factor $\Gamma$ between the guided mode and the QWs, and hence the optical intensity in the active region for fixed input power. To illustrate the associated tradeoffs, in Fig. 1(b) we plot the normalized intensity profile of the fundamental TM mode versus position along the ridge symmetry axis [the dashed line in Fig. 1(a)] for $w_c = 0.3$, $0.6$, and $1$ μm. These curves were obtained from a 3D mode calculation based on the beam propagation method. As evidenced by these simulations, the chosen value of $w_c = 0.6$ μm (close to the wavelength of 1.55-μm light in GaN) gives a relatively narrow mode profile peaked near the QWs and at the same time negligible intensity ($\sim 10^{-3}$ times its peak value) at the sapphire-AlN interface. The corresponding overlap factor with the wells is $\Gamma = 5.3$ %, which is estimated to be a factor of $\sim 3$ to 10 larger than in the various structures of refs. [11-12]. Finally, in a previous study of ISB absorption in GaN/AlN QWs we have found that growth on AlN templates is in general beneficial to the QW structural quality as it does not result in any tensile strained layers whose strain relaxation can lead to the formation of cracks [8]. This allows using a relatively large number of QWs (30 in this work) which contributes to produce a large overlap factor $\Gamma$.

The material growth was carried out by RF plasma-assisted MBE. After nitridation of the sapphire surface and deposition of the AlN template at 870 ºC, the QWs were grown at a lower temperature of 770 ºC and under conditions of slightly excess group-III flux (Ga or Al) to promote 2D growth. Since Al atoms are not readily desorbed from the surface at this temperature, growth interruption under nitrogen flux was performed after the deposition of each AlN layer to consume the excess Al accumulated on the surface. A small flux of In was

also used during growth of the AlN layers because of the beneficial role played by In as a surfactant. All the GaN wells were doped n-type with Si at a nominal level of $4 \times 10^{19}$ cm$^{-3}$.

The QW layer thicknesses were selected so as to yield an energy separation between the ground-state and first-excited conduction subbands close to 1.55 μm. To that purpose, the QW conduction-band structure was modeled using a self-consistent Poisson and Schrödinger equations solver based on the effective-mass approximation. The characteristic built-in electric fields of GaN/Al(Ga)N QWs due to spontaneous and piezoelectric polarizations are included explicitly in this design code following, e.g., Ref. [17]. The right inset of Fig. 2 shows the calculated conduction-band lineup and squared envelope functions of the lowest two subbands of the designed structure: the corresponding ISB transition energy is 805 meV.
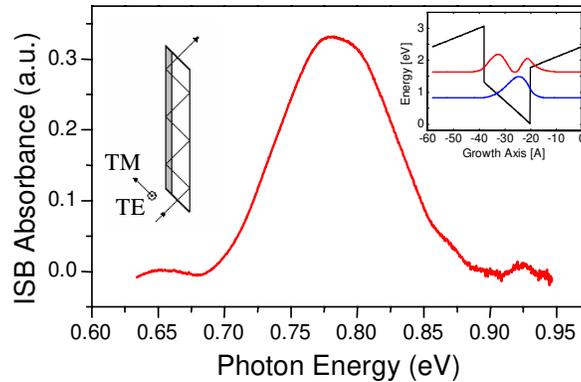


Fig. 2. Measured ISB absorption spectrum of the QW active material used in this work. Right inset: QW conduction-band structure. Left inset: experimental sample geometry.

Shown in Fig. 2 is the ISB absorption spectrum of a small (~ 4x6 mm$^2$) sample from the grown material measured with a Fourier transform infrared (FTIR) spectrometer. The sample was mirror polished on the substrate side and lapped at 45º on two opposite facets to create a multi-pass wedge geometry, as illustrated in the left inset of the figure. Its absorption spectrum was obtained from a TM-polarized transmission spectrum normalized with a TE-polarized spectrum to subtract off background features (given that ISB transitions only couple to TM light). The ISB absorption peak in this figure is centered at about 786 meV (1.58 μm), in fairly good agreement with the design value of 805 meV. Its spectral width is about 97 meV, which is a typical value for near-infrared ISB absorption features in GaN/AlN QWs although a linewidth as small as 40 meV has been reported recently [9].

Ridge waveguides based on this material were fabricated by photolithography and inductively coupled plasma etching using chlorine. Bars containing several waveguides of different widths were finally separated after scribing through the backside. Generally high-quality facets were obtained with this procedure despite the lack of common cleavage planes between the c-plane sapphire substrate and the nitride epitaxial film.

## 3. Waveguide characterization and discussion

For optical testing the waveguides were mounted under a video magnification system, and light was coupled in and out using tapered fibers placed on 5-axis nanopositioning flexure stages. The light source was a passively mode-locked fiber laser. At the waveguide input we used a polarization-maintaining dispersion-shifted tapered fiber to allow control of the input polarization and to avoid excessive broadening of the optical pulses. A variable beam splitter based on free-space polarization optics was used to vary and monitor the input power without changing the laser pumping conditions and hence the pulse temporal and spectral widths.

The coupling and non-saturable propagation losses were measured using the cutback method, with waveguides identical to the structure described in the previous section except for the presence of thinner QWs that do not provide any ISB absorption near 1550 nm. In Fig. 3

we plot the measured fiber-to-fiber transmittance at 1550 nm for TE (circles) and TM (squares) light, from a batch of 14 such waveguides with lengths varying between 1 and 4 mm. These data did not exhibit any dependence on input power, which confirms the non-saturable nature of the propagation losses of these devices. The spread of values measured from waveguides of equal length is likely due to variations in the facet angles and hence in the coupling efficiency. The straight lines in the figure are least-squares fits to the experimental data: from their slopes and vertical-axis-intercepts we extrapolate propagation losses of ~2 (4) dB/mm for TE (TM) light and coupling losses of ~6 dB/facet for both polarizations.
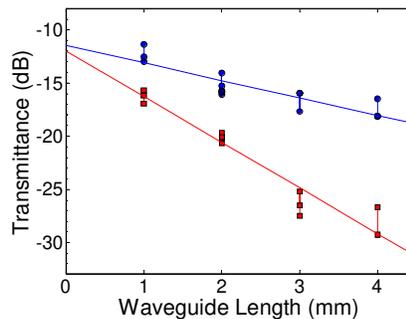


Fig. 3. Measured TE (circles) and TM (squares) transmittance versus waveguide length.

These measured non-saturable propagation losses are relatively small and fully suitable for the present application. Further improvements can be obtained by optimizing the etching conditions so as to minimize sidewall roughness. The 2 dB/mm excess TM losses can be at least partly ascribed to charged edge dislocations parallel to the growth axis which effectively act as a wire-grid polarizer [12]. It should be mentioned that values of such excess losses as large as > 10 dB/mm have been measured in previously developed III-nitride QW waveguides fully grown by MBE [12], which confirms the effectiveness of the present waveguide design as well as the high structural quality of our QW active layer. Our measured coupling losses are also suitable for this application although smaller values of ~ 3-4 dB/facet have been reported [16, 11, 12], and can be improved, e.g., with the use of anti-reflection coatings [11].

To illustrate the nonlinear saturation properties of waveguides based on the QW material of the previous section, in Fig. 4 we plot the measured transmittance at 1550 nm versus in-fiber input average power for three 1-mm-long such devices, with 3-, 5-, and 7-μm ridge widths. As shown in this figure, TM-polarized pulses of sufficiently high power experience substantial self-absorption saturation as they propagate through the waveguides. Vice versa, as illustrated in Fig. 4(a) for the 5-μm-wide waveguide, the TE transmittance is essentially constant with input power, which confirms the ISB origin of the observed nonlinear saturation. The measured increase in TM transmittance is as large as 15 dB in Fig. 4(c), limited by the laser source in our setup.

The input average powers (measured before coupling into the waveguides) required for 3-dB saturation are -3.7, -7.0, and -4.2 dBm for the 3-, 5-, and 7-μm-wide devices, respectively. Given that the pulses coupled into the waveguides have repetition rate of 20 MHz and temporal width of 240 fs (as measured by autocorrelation after an identical fiber span), these values correspond to 3-dB saturation peak powers of approximately 89, 42, and 80 W. We emphasize that these results represent a significant improvement over the best previously reported values of ~190 W (25-pJ saturation pulse energy with 130-fs pulses) for waveguides grown on MOCVD GaN templates, and ~415 W (54-pJ saturation pulse energy with 130-fs pulses) for devices fully grown by MBE such as ours [11,12]. These improvements are mainly due to the larger overlap factor $\Gamma$ between the guided beam and the QWs allowed by our waveguide design, and to the lower non-saturable TM excess losses (relative to previous fully MBE-grown devices). The QW structural quality is also important in this respect, although the material ISB saturation intensity inferred from our measurements (on the order of

a few W/$\mu m^2$) is comparable to previous reports [6]. The observed increase in saturation power as the ridge width is increased from 5 to 7 $\mu$m is qualitatively consistent with the corresponding increase in modal area. On the other hand, the larger value measured as the width is decreased to 3-$\mu$m is likely due to an increase in coupling losses with narrower waveguides, which is confirmed by other loss measurements.
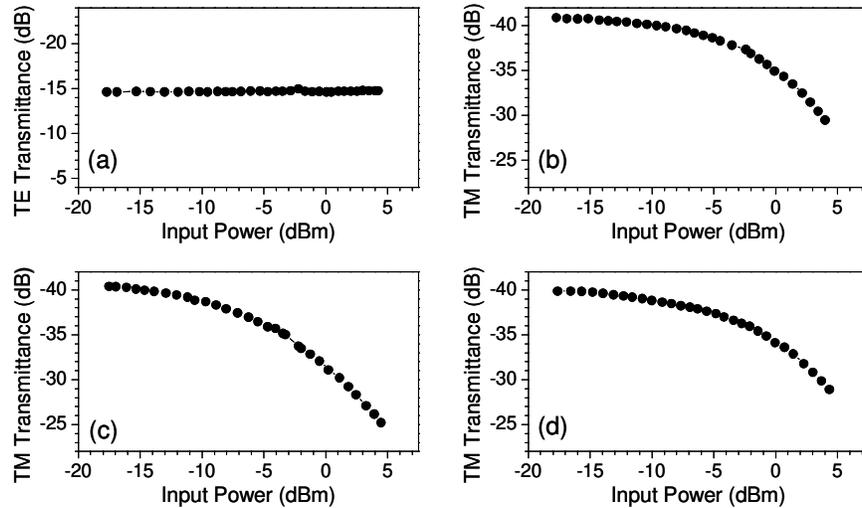


Fig. 4. TE (a) and TM (b-d) transmittance versus in-fiber input average power for a 3-$\mu$m (b), 5-$\mu$m (a, c), and 7-$\mu$m (d) wide waveguide.

Regarding the magnitude of the ISB absorption losses extrapolated from the data of Figs. 3 and 4 [e.g. ranging from ~24 to ~9 dB in Fig. 4(c)], they are comparable with previous reports [11, 12]. These losses, and hence the overall TM transmittance, can be varied to meet given specifications by varying the waveguide length. In particular, the optimal length can be determined based on a tradeoff between the smallest achievable on-state losses and the largest achievable contrast ratio. On the other hand, the 3-dB saturation power is largely length independent over a wide range of length values, since the shorter the waveguide the larger the average ISB absorption saturation for fixed input power, but at the same time the smaller the overall transmission loss saturation for fixed ISB absorption saturation. This expectation is confirmed by simulations of light propagation in these nonlinear waveguides.

## 4. Summary

In conclusion, we have demonstrated nonlinear optical waveguides based on ISB transitions in GaN/AlN QWs, which exhibit record low values of the saturation power. This important parameter can be further decreased by improving the input coupling efficiency and propagation losses, and by using more complex QW structures. In particular, as shown numerically in Ref. [15] properly designed AlGaN coupled QWs can be used to reduce the ISB absorption saturation intensity by a factor of over 30. Altogether we can therefore expect that 3-dB saturation peak powers of less than 1 W (i.e. 3-dB saturation pulse energies of less than 1 pJ using sub-picosecond pulses) can be achieved. Combined with their ultrafast absorption recovery lifetimes, ISB transitions in III-nitride QWs are therefore very promising for all-optical signal processing applications in future ultra-broadband communication networks.